Mon. Not. R. astr. Soc. (1988) **233**, 667–676

Crab Pulsar timing 1982–87

A. G. Lyne, R. S. Pritchard and F. G. Smith *University of Manchester, Nuffield Radio Astronomy Laboratories, Jodrell Bank, Macclesfield, Cheshire SK11 9DL*

Accepted 1988 February 8. Received 1988 February 8; in original form 1987 November 27

Summary. We present observations of the arrival times of pulses from the pulsar in the Crab Nebula over a six-year interval. The data are intended to permit the investigation of the interior of the neutron star through the study of glitches and timing noise and to provide an ephemeris for high-energy observations. The first and second frequency derivatives provide a value for the braking index of $n=2.509\pm0.001$, which is consistent with previous observations. The third frequency derivative can now be determined over an 18-yr span and is as expected for this braking index. The predominant deviations from a simple slow-down model form a sinusoid with a period of 20 months, attributable to an oscillation of the bulk of the neutron superfluid in the pulsar. One conspicuous glitch occurred in 1986 August, and the subsequent recovery was studied from only one hour after the event.

1 Introduction

The rotation of the Crab Pulsar, PSR 0531+21, has previously been monitored on a more or less continuous basis over the decade 1969–79. Demianski & Proszynski (1983) presented an analysis of the complete run of data, combining optical data from Groth (1975) and from Lohsen (1981) with radio data from Gullahorn *et al.* (1977). They noted with regret that these sets of observations had all ended leaving unanswered several questions on the occurrence and nature of timing irregularities. Our own radio observations, which provide almost daily timing since early 1982, were intended both to address these questions and to provide an ephemeris for other observations, particularly in the gamma-ray region.

This paper sets out our observational methods and the data reduction techniques which lead to the ephemerides which we have been providing since 1982 (Lyne & Smith 1982). We also follow Demianski & Proszynski in analysing the arrival times to find the variations in rotation rate ν and its first derivative ν' over the six years 1982–87, and explore the deviations in pulse phase from a simple model of rotation in which single values of the rotation frequency ν and its derivatives ν' and ν'' are fitted to the complete run of data.

2 Observational method

A 12.5-m diameter radio telescope sited at Jodrell Bank is used for most of the observations. It is equipped with a low-noise receiver at 610 MHz, bandwidth 4 MHz, detecting both hands of circular polarization. Observations at radio wavelengths have the advantage over those at optical wavelengths in that they can be continued throughout the year, regardless of daylight or the weather. They may suffer, however, from any variability in interstellar dispersion or multipath scattering. Measurements on two or more different radio frequencies are required to evaluate and remove these effects. For this reason, occasional observations are made at other radio frequencies, 327, 408, 930, 1420 or 1667 MHz, either with the 12.5-m, with the 76-m Lovell Telescope or with one of the MERLIN telescopes, so that the dispersion measure and interstellar scattering of the radio pulses can be determined (see Section 3).

Over the finite bandwidth which is needed for sufficient sensitivity, there are large effects arising from the dispersion in the interstellar medium. We therefore divide the 4-MHz total RF band into 32 contiguous channels which are separately detected. The outputs are sampled, digitized and added together with time delays appropriate for the dispersion measure of the pulsar. The sampling interval is 260 μs at 610 MHz. Subsequent profile fitting and integration (see Section 3) leads to a typical accuracy in arrival time of 20 μs in a 10-min integration, so we have ensured that the stability of the sampling technique is at least sufficient for such accuracy. In the event that one of the remote radio telescopes of the MERLIN network is used, the undetected signal is transferred by microwave link to Jodrell Bank for processing. We take due account of the propagation delay over the radio link in calculating an arrival time.

The observatory rubidium clock is calibrated regularly against the European Loran C transmission. This permits the observations to be related to UTC with an error of less than 10 μs.

The integration time for a single observation is usually 5 or 10 min. Wherever possible the observations are continued over about 14 hr each day. They are recorded on magnetic tape, and usually sections about 2 hr in length are selected for timing analysis from the beginning and end of each 12-hr run.

3 Matching the pulse profile

The on-line signal integration over intervals of 5 or 10 min which leads to an observed profile relies on a sufficiently accurate predicted value of the observed period, which is available from our own ephemeris for the pulsar, and a simple ephemeris for the velocity of the Earth. The actual arrival time, or phase, of the main pulse is found by matching the observing pulse profile with a template. This template is constructed from a model of the whole pulse profile, including the precursor component and the interpulse, whose amplitudes relative to the main pulse depend on the observing frequency.

The model is also elaborated to take account of interstellar scattering, which results in the lengthening of the pulse components and delays their centroids. The scattering apparently originates partly in the interstellar propagation path and partly in the Crab Nebula itself. This latter component is very variable (Lyne & Thorne 1975) and we attempt to evaluate it every month by direct inspection of the observed profile at 408 MHz. The most obvious effect of scattering is to convolve the unscattered pulse with a function which to first order is a truncated exponential, giving rise to an exponential tail on both the main pulse and the interpulse. We therefore fit an exponential function to the part of this tail more than 200 μs from the peak of the main pulse, and use the value of the exponent to construct the template. Higher frequency observations indicate that any power more than 200 μs after the peak is probably scattered radiation and not part of the intrinsic pulse profile. Trials show that in this way the delay of the

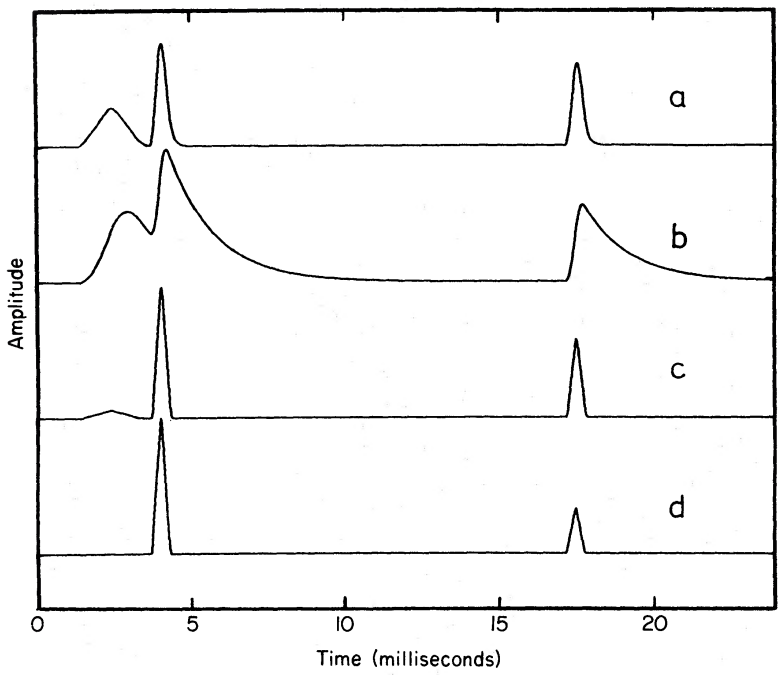

Figure 1. Four examples of profile templates, showing the effects of spectral differences between the components and interstellar scattering. (a) 408 MHz with scattering of 100 μs, (b) 408 MHz with scattering of 1000 μs, (c) 610 MHz and (d) 1420 MHz.

pulse arrival time is corrected for this effect to within about 10 per cent of the exponential decay time, which is typically 100 μs or less at 408 MHz.

Examples of some templates are shown in Fig. 1, including one in which the effects of scattering are severe.

4 The barycentric correction and the ephemeris

The correction of the observed arrival times to barycentric arrival times and infinite frequency follows established techniques and uses either the MIT ephemeris PEP 311 (Ash, Shapiro & Smith 1967) or the JPL ephemeris DE 200 (Standish 1982). Over intervals of about one month, we perform least-squares fits to the data to obtain best values for the dispersion measure (DM), the arrival time at infinite frequency, the period and the rate of change of period, and tabulate these for distribution (Lyne & Smith 1982). The subsequent analysis in this paper utilizes the JPL ephemeris and the results are presented in Table 1 in terms of rotation frequency ν and its derivative, rather than the period P.

5 Dispersion and scattering

The values of dispersion measure, derived from the least-squares fitting procedure, and a scattering parameter are given in the table. The scattering parameter is simply the exponent in the scattering tail observed at 408 MHz. If derived from other frequencies, the value was scaled as (frequency)$^{-4}$.

The quoted values of dispersion measure are believed to be accurate to within 0.005 pc cm^{-3}. The graph of monthly values (Fig. 2) shows a slow variation and step changes, both of magnitude approximately 0.02 pc cm^{-3}, i.e. 3×10^{-4} of the total DM. These variations amount to a total change of 6×10^{16} cm^{-2} in electron content: these are presumably attributable to changes along the

Table 1. Monthly timing results for PSR 0531+21, 1982–87.

DATE		MJD	ARRIVAL TIME (sec) (MIT)	ARRIVAL TIME (sec) (JPL)	FREQUENCY (Hz)	ERROR	FREQDOT (10^{-15}sec^{-2})	ERROR	DM (pc cm^{-3})	SCAT408 (μsec)	EPHA((μsec
		Note(1)	Note(2)	Note(3)	Note(4)		Note(5)		Note(6)	Note(7)	Note(
FEB	82	45015	0.014468	0.007409	30.0592240994	3	-381010.63	0.87	56.836	100	100
MAR	82	45043	0.012550	0.005426	30.0583024249	2	-380959.44	0.59	56.839	100	100
APR	82	45074	0.021132	0.014105	30.0572820742	8	-380936.18	1.38	56.831	100	50
MAY	82	45104	0.003367	0.029891	30.0562947409	12	-380915.08	2.66	56.824	100	175
JUN	82	45135	0.017696	0.011046	30.0552745667	20	-380832.86	5.47	56.826	100	500
JUL	82	45165	0.006709	0.000438	30.0542874262	2	-380820.64	0.59	56.827	100	60
AUG	82	45196	0.023044	0.017022	30.0532674731	4	-380800.82	1.31	56.825	100	50
SEP	82	45227	0.031304	0.025770	30.0522475686	6	-380777.52	0.70	56.838	100	500
OCT	82	45257	0.007924	0.001825	30.0512606830	21	-380759.37	5.33	56.827	100	500
NOV	82	45288	0.010390	0.004128	30.0502409274	6	-380714.83	0.85	56.831	100	70
DEC	82	45318	0.023396	0.016729	30.0492541575	16	-380684.64	1.63	56.800	100	50
JAN	83	45349	0.026736	0.019665	30.0482345788	3	-380657.72	0.75	56.809	100	80
FEB	83	45380	0.021747	0.014489	30.0472150799	3	-380610.37	1.18	56.807	100	80
MAR	83	45408	0.023021	0.015648	30.0462943343	4	-380579.28	0.67	56.814	100	60
APR	83	45439	0.000604	0.026644	30.0452750240	4	-380553.41	1.26	56.820	100	60
MAY	83	45469	0.017017	0.009935	30.0442886507	2	-380522.61	0.60	56.811	100	60
JUN	83	45500	0.021461	0.014712	30.0432695111	1	-380483.65	0.33	56.819	100	60
JUL	83	45530	0.005403	0.032245	30.0422833396	1	-380459.82	0.42	56.826	100	60
AUG	83	45561	0.003698	0.030775	30.0412643519	1	-380430.09	0.44	(56.825)	100	60
SEP	83	45592	0.006932	0.000776	30.0402454496	1	-380398.71	0.34	56.814	100	50
OCT	83	45622	0.026632	0.020421	30.0392595092	2	-380362.70	0.57	56.827	100	100
NOV	83	45653	0.014812	0.008284	30.0382407722	2	-380327.06	0.58	56.827	100	60
DEC	83	45683	0.031058	0.024209	30.0372549969	5	-380311.32	1.08	56.827	100	150
JAN	84	45714	0.008465	0.001257	30.0362364246	1	-380260.40	0.40	56.816	100	50
FEB	84	45745	0.018300	0.010832	30.0352179657	1	-380231.04	0.22	56.822	100	50
MAR	84	45774	0.030814	0.023258	30.0342653036	1	-380196.39	0.35	56.829	100	60
APR	84	45805	0.015263	0.007794	30.0332469984	3	-380175.45	0.70	(56.825)	100	60
MAY	84	45835	0.009586	0.002343	30.0322616421	2	-380134.89	0.48	(56.825)	100	50
JUN	84	45866	0.005599	0.031919	30.0312435446	3	-380097.01	0.63	56.825	200	80
JUL	84	45896	0.023929	0.017301	30.0302583496	2	-380076.97	0.47	56.833	200	80
AUG	84	45927	0.000026	0.027063	30.0292404093	4	-380048.22	1.16	56.826	720	120
SEP	84	45958	0.021984	0.015565	30.0282225402	11	-379996.32	1.96	56.837	1100	100
OCT	84	45988	0.010088	0.003585	30.0272376130	7	-379981.24	1.32	56.845	1600	200
NOV	84	46019	0.033011	0.026230	30.0262199188	5	-379955.96	1.12	56.845	1500	700
DEC	84	46049	0.009307	0.002075	30.0252351314	8	-379919.24	2.24	56.828	130	200
JAN	85	46080	0.006919	0.032654	30.0242175961	3	-379884.59	1.07	56.829	200	50
FEB	85	46111	0.012592	0.004880	30.0232001507	2	-379856.01	0.63	56.829	200	40
MAR	85	46139	0.003200	0.028706	30.0222812475	2	-379819.09	0.49	56.834	200	30
APR	85	46170	0.011903	0.004126	30.0212639685	10	-379792.49	0.28	56.830	100	25
MAY	85	46200	0.031314	0.023809	30.0202795691	8	-379771.06	2.30	56.828	100	30
JUN	85	46231	0.009932	0.002752	30.0192624486	2	-379730.43	0.57	56.832	100	50
JUL	85	46261	0.019567	0.012684	30.0182782377	3	-379701.56	0.82	56.832	100	60
AUG	85	46292	0.002711	0.029368	30.0172612827	3	-379662.41	0.70	56.847	100	100
SEP	85	46323	0.007760	0.001157	30.0162444749	98	-379624.97	11.27	(56.840)	100	75
OCT	85	46353	0.026745	0.020095	30.0152604966	3	-379603.62	0.66	56.824	100	50
NOV	85	46384	0.021464	0.014482	30.0142438237	1	-379562.60	0.25	56.826	100	40
DEC	85	46414	0.021863	0.014554	30.0132600400	2	-379530.75	0.84	(56.826)	100	75
JAN	86	46445	0.009653	0.001941	30.0122435431	1	-379494.99	0.40	56.803	100	40
FEB	86	46476	0.012655	0.004686	30.0112271265	1	-379471.57	0.30	56.803	100	40
MAR	86	46504	0.003431	0.028676	30.0103091562	2	-379442.23	0.46	56.807	100	50
APR	86	46535	0.001428	0.026756	30.0092929040	1	-379411.89	0.36	56.805	100	40
MAY	86	46565	0.011422	0.003653	30.0083095099	4	-379363.63	1.17	56.808	100	150
JUN	86	46596	0.029908	0.022463	30.0072934309	5	-379333.68	2.17	(56.808)	100	100
JUL	86	46626	0.019031	0.012089	30.0063102177	2	-379318.56	0.46	(56.808)	100	50
AUG	86	46657	0.028521	0.021633	30.0052942758	3	-379287.23	0.65	(56.808)	100	60
SEP	86	46688	0.033026	0.026209	30.0042784461	2	-379280.40	0.43	56.846	100	700
OCT	86	46718	0.008827	0.001897	30.0032954435	1	-379229.51	0.27	56.834	100	120
NOV	86	46749	0.032338	0.025118	30.0022797696	6	-379182.47	1.45	56.846	100	80
DEC	86	46779	0.018592	0.011005	30.0012969454	1	-379159.42	0.30	56.849	100	20
JAN	87	46810	0.026030	0.018029	30.0002814571	2	-379130.09	0.40	56.848	100	60
FEB	87	46841	0.025959	0.017671	29.9992660523	2	-379096.67	0.61	56.847	100	100
MAR	87	46869	0.021463	0.013074	29.9983489891	6	-379057.52	2.36	56.854	100	120
APR	87	46900	0.010824	0.002518	29.9973337608	3	-379031.90	0.62	(56.854)	100	70
MAY	87	46930	0.014836	0.006773	29.9963513383	2	-379014.44	0.56	56.854	100	60
JUN	87	46961	0.014888	0.007172	29.9953362531	5	-378971.53	1.36	56.861	100	140
JUL	87	46991	0.029113	0.021737	29.9943540177	4	-378932.94	1.16	(56.862)	1500	125
AUG	87	47022	0.008901	0.001783	29.9933391125	3	-378893.69	0.85	(56.862)	750	100
SEP	87	47053	0.027060	0.020027	29.9923243185	4	-378880.41	1.03	56.862	1000	100

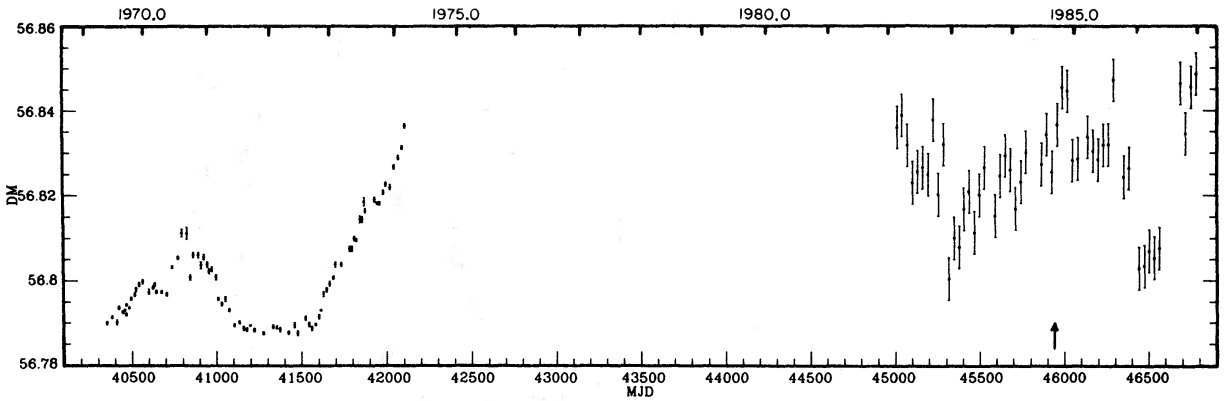

Figure 2. The variation in dispersion measure over the period 1969–87. Data for the years 1969–75 are taken from Isaacman & Rankin (1977).

line-of-sight within the Crab Nebula. The increased scattering at MJD 45950 may be associated with a small increase of DM, indicated by an arrow in the figure. This figure does not include the conspicuous variations in DM which occur over a few days in June each year when the pulsar is observed through the solar corona; few observations were made when the pulsar was within 5° of the Sun. The maximum effect close to the Sun amounts to about 500 μs at 610 MHz, corresponding to an increase in DM of 0.045 pc cm^{-3} or of 1.4×10^{17} cm^{-2} in the total electron content.

Two major changes in scattering were recorded, from 1984 August to November and from 1987 July to October. These are similar in magnitude and duration to the major event of 1974, which lasted for 4 months (Lyne & Thorne 1975).

6 Analysis of the 6-yr run of data

Our set of data is more consistent and more closely sampled than the previous sets analysed by Demianski & Proszynski (1983). Following their analysis, we divided our data set into monthly subsets and found best-fitting values for ν and ν' for each. These values are given in Table 1. In Fig. 3(a) we plot the monthly values of ν' and in Fig. 3(b) the values after subtracting a linear variation, i.e. allowing for a constant value of ν''. Data from the previous analysis by Demianski & Proszynski, covering the decade 1969–79, are included. The well-known step in 1975 February is

---

otes:

1. Modified Julian Date (MJD) is the Julian Date – 2400000.5.
2. The arrival time is that of the centre of the first main pulse after midnight at infinite frequency at the barycentre of the Solar ystem, in seconds. The time-scale is TAI. 32.184 s must be added to convert to TDB. Position used for reductions: RA (1950.0) $^{h}31^{m}31\overset{s}{.}4060$, Dec. (1950.0) +21° 58′ 54″.391. The MIT barycentric ephemeris (PEP311) was used.
3. The arrival time obtained using the JPL (DE200) ephemeris.
4. The observed barycentric frequency is given at the quoted arrival time.
5. The observed derivative of the barycentric frequency is given at the quoted arrival time.
6. The observed dispersion measure is usually given, the error being about 0.005 pc cm^{-3}. If the value given is in parenthesis, then is is an assumed value, extrapolated from adjacent data.
7. The assumed delay due to interstellar scattering is given for 408 MHz. It is assumed to scale as (frequency)$^{-4}$.
8. The quoted accuracy is that with which the ephemeris defined from these data is believed to describe the observed arrival times uring the month.
9. The end of the fit for 1986 August and the beginning of the fit for 1986 September is taken as MJD 46664.0, that is midnight on 86 August 22. This is the date of a significant glitch (Lyne & Pritchard 1987).

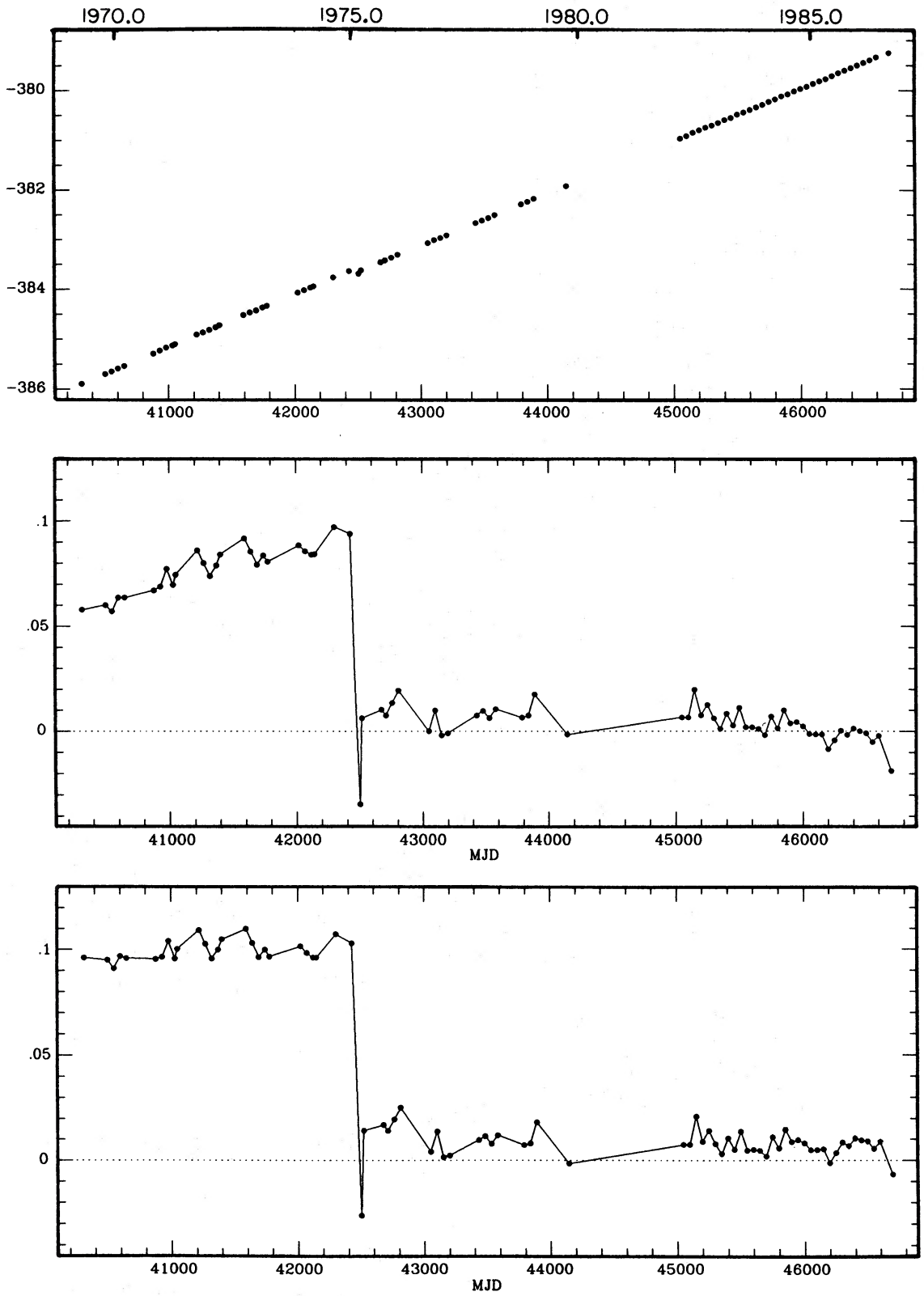

Figure 3. (a) First derivative ν' obtained from monthly fits for the years 1969–87, (b) after subtracting a linearly increasing value of ν', i.e. a constant value of $\nu''=1.208\times10^{-2}\,s^{-3}$, and (c) as (b) but using the predicted value of $\nu'''=-0.61\times10^{-30}\,s^{-4}$.

evidently the only such major occurrence in the frequency, although smaller deviations can be seen which are not explicable by noise in the receiving system.

The constant value of ν'' used in data reduction for Fig. 3(b) is $\nu''=1.208\times10^{-20}\,s^{-3}$. The braking index n in the rotation slowdown law

$$\nu' \propto -\nu^n$$

is related to ν'' by

$$n=\frac{\nu\nu''}{\nu'^2}.$$

Our value of ν'' gives $n=2.509\pm0.001$.

There is an appreciable curvature in Fig. 3(b), indicating that the third derivative ν''' is measurable. The slow-down law leads us to expect

$$\nu'''=\frac{n(2n-1)\nu'^3}{\nu^2}=-0.615\times10^{-30}\,s^{-4}.$$

Fig. 3(c) shows the same data set after allowing for this theoretical value. Our observations evidently agree with this value to about 10 per cent, providing further support for the simple exponential slow-down model.

We now study the irregularities in rotation which remain after allowing for these best-fitting values of rotation frequency ν and its derivatives ν' and ν''. The fitting of these parameters for the complete 6-yr run of data results in the deviations of arrival time shown in Fig. 4. We have also applied the value of ν''' as determined above from the 18-yr data span. Evidently every rotation of the 5×10^9 during this period has been accounted for, and the deviations do not exceed 15 ms, i.e. half of a rotation period.

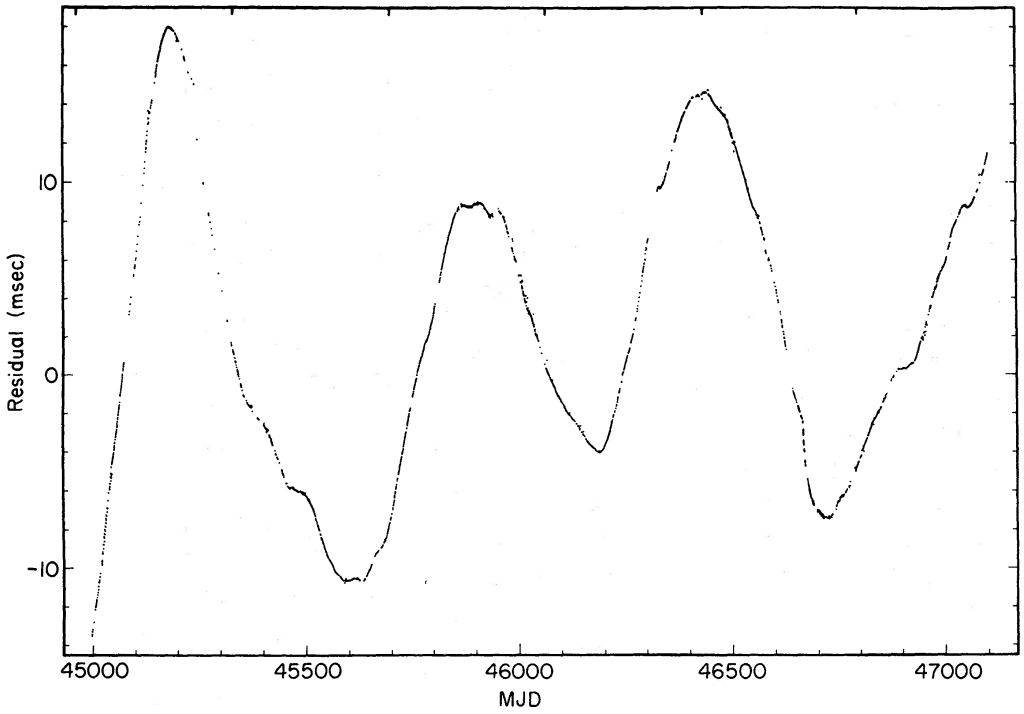

Figure 4. Deviations in arrival times from a single best-fitting model covering the whole six-year period. A single value of 56.825 pc cm^{-3} was assumed for the dispersion measure and one of 100 μs for the interstellar scattering at 408 MHz.

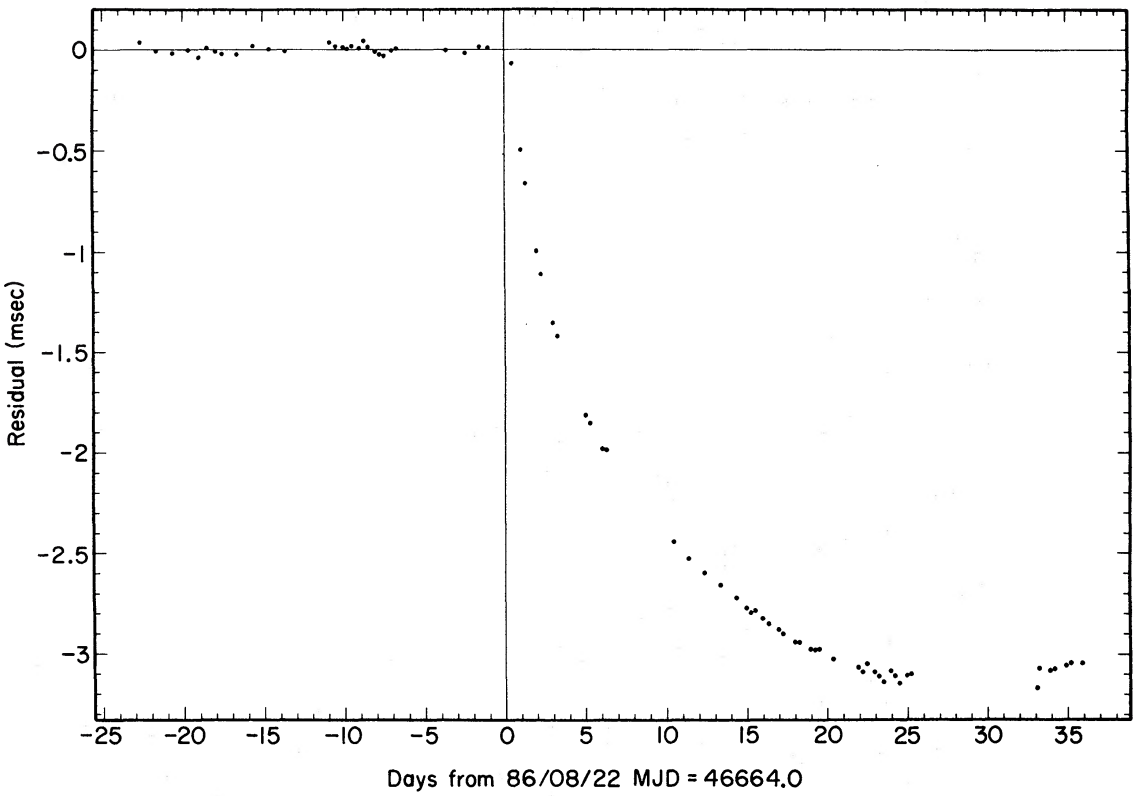

Figure 5. The glitch of 1986 August. The timing data over a period of 60 days before the glitch were used to establish a model for ν and ν' from which the timing deviations were measured.

We have searched for other glitches by expanding the scale of the phase deviations in Fig. 4. The only well-defined event can be discerned on 1986 August 22 (MJD 46664.4). The progress of this glitch was monitored in unprecedented detail; it appears that it occurred one hour before observations began (Fig. 5). Details have been published separately by Lyne & Pritchard (1987). The amplitude of the phase deviation was about 3 ms, and the recovery time constant was about 5 days.

There have been two earlier well-defined glitches in the Crab Pulsar, in 1969 and 1975. These were originally discussed by Boynton *et al.* (1972) and by Gullahorn *et al.* (1977). Alpar *et al.* (1984, 1985) have successfully interpreted these events in terms of the 'vortex creep' model, in which the coupling between the crust of a neutron star and part of its superfluid interior is disturbed catastrophically. In a steady state, the vortices in the superfluid, which represent its rotation, creep outwards through the crystal lattice of the crust, the rate of creep depending on the slow-down rate of the pulsar and on the energetics of the pinning process which tends to attach the vortices to the nuclei. The net rotation of the superfluid is greater than the rotation rate of the crust. At the moment of the glitch, a number of vortices move rapidly outwards and pin to the crust. The subsequent recovery represents a re-establishment of the vortex creep.

The characteristics of the 1986 August glitch show that the effective total moment of inertia of the neutron star decreased by 0.4 per cent at the moment of the glitch: this presumably represents those vortices which were newly pinned to the crust. The recovery curve is a very good exponential for the whole run of observations from one hour after the glitch until 40 days later when most of the period perturbation has been recovered. The observations after this time fit a straight line, i.e. the period is constant apart from the long-term slowdown. The minor change in slope occurring at MJD 46754 represents only a few per cent of the change of period at the glitch and is

not dissimilar to many events occurring during the six years. No further exponential recovery can be seen.

7 The quasi-sinusoidal deviations

The outstanding feature of the deviations in arrival time shown in Fig. 4 is a quasi-sinusoidal oscillation with a period of approximately 20 months. Previous analysis of the earlier data sets, by Groth (1975), Cordes (1980) and Boynton (1981), treated the waveform of the deviations as a random function of time, seeking to evaluate the spectrum of the random noise components which it contained. Our consistent set of data allows us to suggest that the spectrum is totally different from random noise.

These previous analyses compared the deviations of observed arrival times from best-fitting models for various lengths of data strings; the model for each fit used independently determined best-fitting values for rotation frequency ν and its first two derivatives ν' and ν''. It was found that the deviations were much larger for data strings a year or more in length than for short strings, and the conclusion was drawn that the noise spectrum was strongly biased to low frequencies.

Our run of data covering nearly six years suggests that the long-time-scale deviations are not noise-like but quasi-periodic. There is a single, dominant frequency component with a 20-month period, whose amplitude varies from 10 to 5 ms. The same periodicity is found in shorter data strings, demonstrating that it is not an artefact of our methods of analysis. We note that this same period appears in the earlier data (Demianski & Proszynski 1983), although there is less evidence for a coherent oscillation. Unfortunately no data are available for the period 1979–81, and the glitch of 1975 disturbed the long-time-scale analysis of the earlier data set; nevertheless, it seems unlikely that a coherent oscillation could have continued over the whole period from 1969 to 1986.

Quasi-periodic deviations also appear in analyses of pulse arrival times from other pulsars which have been monitored over periods of 5–10 yr by Cordes & Downes (1985) and by Manchester *et al.* (1983). These may not all be truly periodic: a single cycle of oscillation covering the whole observation period is equally well represented as the effect of an unexpectedly high value of ν'', as seen during the recovery from a glitch. Others are not so easily explained, and it is possible that many pulsars with periods of order 500 ms show oscillations with periods of around 5 yr.

A regular periodic deviation in any of these pulsars could be produced by a planet with several Earth masses orbiting the pulsar. The existence of such a planet seems unlikely; furthermore, the observed deviations are too far removed from the expected regular behaviour for this possibility to be considered likely. We prefer to seek an explanation in the internal structure of the pulsar.

Any internal oscillation with such a long period must involve the neutron superfluid which is the main constituent of the neutron star interior. Rotation in this superfluid is manifested as quantized vortices, as in rotating liquid helium. Oscillation in a regular structure of vortices has been investigated by Tkachenko (1966); he showed that the periodicity of such oscillations depends on the linear scale of the rotator and on the square root of the rotation period. Ruderman (1970) and Lamb, Pines & Shaham (1978) find that the expected period P_{TK} of Tkachenko oscillations for a neutron star rotating with Period P_{rot} (s) is

$$P_{TK}=20\,R_6\,P_{rot}^{1/2} \text{ month}$$

where R_6 is the radius in units of 10^6 cm. This prediction leads to periods which are too short by a factor of 5. Nevertheless, it may be significant that the oscillations in longer-period pulsars, if they exist, appear at longer periods as expected from the Tkachenko proposal.

We therefore propose that the superfluid cores of pulsars can oscillate about a mean angular position determined by the crust. The oscillations may well be initiated by a glitch, although this is

difficult to ascertain in the existing data. The coupling between the core and the crust is at present considered to be very tight, because of the interaction between the crust magnetic field and the core vortices via the charged components of the neutron superfluid (Easson 1979); it may be necessary to reconsider this analysis in the light of the core oscillations which are indicated by our timing data.

8 Conclusions

This programme of radio monitoring, which runs largely automatically, provides a consistent set of data throughout the year, covering most of the time that the Crab Pulsar is above the horizon at Jodrell Bank. Ephemerides for the rotation of the pulsar on a monthly basis are available on request for use by other observers.

Analysis of a six-year data set shows that all arrival times fit a simple model within half the pulsar rotation period; the predominant deviations during this series of observations form a sinusoid with a period of 20 months. These deviations appear not to be an artefact of our methods of data reduction, and we attribute them to an oscillation of the main bulk of the neutron superfluid in the pulsar. A third conspicuous glitch occurred in 1986 August; our observations trace the recovery in detail from only one hour after the event.

These observations are continuing with the purpose of following the development of the oscillation and studying in detail any future glitches.

References

Alpar, M. A., Nandkumar, R. & Pines, D., 1985. *Astrophys. J.*, **288,** 191.
Alpar, M. A., Anderson, P. W., Pines, D. & Shaham, J., 1984. *Astrophys. J.*, **276,** 325.
Ash, M. E., Shapiro, I. I. & Smith, W. B., 1967. *Astr. J.*, **72,** 338.
Boynton, P. E., 1981. *IAU Symp. No. 95,* 279.
Boynton, P. E., Groth, E. J., Hutchinson, D. P., Nanos, G. P., Jr., Partridge, R. B. & Wilkinson, D. T., 1972. *Astrophys. J.*, **175,** 217.
Cordes, J. M., 1980. *Astrophys. J.*, **237,** 216.
Cordes, J. M. & Downes, G. S., 1985. *Astrophys. J. Suppl.*, **59,** 343.
Demianski, M. & Prozynski, M., 1983. *Mon. Not. R. astr. Soc.*, **202,** 437.
Easson, I., 1979. *Astrophys. J.*, **228,** 257.
Groth, E. J., 1975. *Astrophys. J. Suppl. Ser.*, **29,** 431.
Gullahorn, G. E., Isaacman, R., Rankin, J. M. & Payne, R. R., 1977. *Astr. J.*, **82,** 309.
Isaacman, R. & Rankin, J. M., 1977. *Astrophys. J.*, **214,** 214.
Lamb, F. K., Pines, D. & Shaham, J., 1978. *Astrophys. J.*, **224,** 969.
Lohsen, E., 1981. *Astr. Astrophys. Suppl. Ser.*, **44,** 1.
Lyne, A. G. & Pritchard, R. S., 1987. *Mon. Not. R. astr. Soc.*, **229,** 223.
Lyne, A. G. & Smith, F. G., 1982. *IAU Circ. No. 3705.*
Lyne, A. G. & Thorne, D. J., 1975. *Mon. Not. R. astr. Soc.*, **172,** 97.
Manchester, R. N., Newton, L. M., Hamilton, P. A. & Goss, W. M., 1983. *Mon. Not. R. astr. Soc.*, **202,** 269.
Ruderman, M. A., 1970. *Nature,* **225,** 619.
Standish, M., Jr., 1982. *Astr. Astrophys.*, **114,** 297.
Tkachenko, V. K., 1966. *Soviet Phys. JETP,* **23,** 1049.